Electronic Supplementary Information

A Novel High-Energy Density Lithium-Free Anode Dual-ion Battery and *In Situ* Revealing the Interface Structure Evolution

Li-Na Wu,[a, b] *Zheng-Rong Wang,*[a, b] *Peng Dai,*[b] *Yu-Xiang Xie,*[b] *Cheng Hou,*[a] *Wei-Chen Zheng,*[b] *Fa-Ming Han,*[c] *Ling Huang,* *[b] *Wei Chen,*[*a] *Shi-Gang Sun*[*b]

[a]Guangxi Key Laboratory of Low Carbon Energy Materials, School of Chemistry and Pharmaceutical Sciences, Guangxi Normal University, Guilin 541004, China

[b]State Key Laboratory of Physical Chemistry of Solid Surfaces, Collaborative Innovation Center of Chemistry for Energy Materials, College of Chemistry and Chemical Engineering, Xiamen University, Xiamen, 361005, China

[c]Guangxi Key Laboratory of Electrochemical and Magneto-chemical Functional Materials, College of Chemistry and Bioengineering, Guilin University of Technology, Guilin 541004, China

Experimental Section

Materials Synthesis: Carbon paper (shanghai, hesenchem, thickness of 190 μm) was cut with a diameter of 16 mm for use as the anode electrode. The graphite cathode was prepared by blending graphite, conductive carbon black, and poly-vinylidene fluoride (PVDF) in N-methyl-2-pyrrolidone (NMP) with a weight ratio of 8:1:1. The above mixture was stirred constantly in a mixed defoamer (THINKY, ARM310) to form a uniform slurry, and then coated onto carbon-coated aluminum foil (Shenzhen Kejingstar) and dried in a vacuum oven at 80 ℃. After that, the dried foil was cut into slice with a wafer slicer (Φ=16mm) for cell assembly.

Electrolytes Preparation: Basically, the base electrolyte (4M $LiPF_6$+EMC+ 3vol% VC+5 vol% FEC) was purchased from Dodochem., LiFSI (Lithium bis(fluorosulfonyl)imide, 99%; from Aladdin) serves as the electrolytic additive. The LiFSI-containing electrolyte was prepared in the argon-filled glove box with moisture and oxygen levels less than 1 ppm.

Cell Fabrication: 2025-type coin cells were fabricated in the argon-filled glove box with moisture and oxygen levels less than 1 ppm. Carbon paper and prepared graphite are used as anode and cathode, respectively. Glass fiber (grade 934-AH, Whatman) serves as the separator.

Characterization and Electrochemical Tests: The assembled cell was charged/discharged galvanostatically on a battery tester (LAND CT2011A) in the voltage range of 3~5 V. The linear sweep voltammogram (LSV) and Tafel test were performed with a three-electrode cell on a CHI660D electrochemical station (Chenhua, China). Pt electrode was used as the working electrode, and Li metal electrodes were used as counter electrode and reference electrode, respectively. The area of the working electrode is 2 cm^2. The cyclic voltammetry (CV) was performed with a 2025 coin-cell on a CHI660D electrochemical station (Chenhua, China) in a voltage range of 3~5 V (vs. Li/Li^+). Graphite electrode and carbon paper were used as cathode and anode, respectively. Nuclear Magnetic Resonance (NMR) spectra are collected on an Avance III HD 500 MHZ NMR. X-ray photoelectron spectroscopy (XPS) was carried out on a Thermo Fisher Scientific K-Alpha. The measurements of ion conductivity were used on ModelDDS-307 Conductometer Instruction. The measurements of viscosity were used on DH2- Rotary rheometer.The Electrochemical Impedance Spectroscopy (EIS) tests were carried out on a Princeton PARSTAT 2263 (USA) with ac current voltage amplitude set as 5 mV and frequency between 100 kHz and 10 mHz. The *in-situ* EIS tests were carried out on an EnergyLab electrochemical workstation with amplitude set as 5 mV and frequency between 100 kHz and 0.1Hz. The corresponding resistance values were fitted

on a zview software. Scanning electron microscope (SEM) images were collected on a HITACHI S-4800 field emission scanning electron microscope (operating at 10 kV). The online continuous flow differential electrochemical mass spectrometry (OEMS) was conducted in a specially designed coin cell (modified 5975C mass selective detector, Agilent). Gas evolution product was detected by helium with a flow rate of 8 mL min^{-1} and then passed through a cold trap (a mixture of dry ice and ethanol, −78.5 ℃ and 1 atm) to condense the electrolyte vapor before entering the mass spectrometer. The *in-situ* X-ray diffraction (XRD) was carried out in a specially designed coin cell by Bruker D8 discover diffractometer. The galvanostatic charging/discharging experiments were performed in a voltage range between 3 ~5 V at 0.2C, and acquisition time of each data in XRD test takes 15 min.

Computational Details: All density functional theory calculations were performed with the Gaussian 16 A.03 program.[1] Geometry optimizations were carried out at the M06-L[2]/def2-TZVP[3] level of theory and frequency calculations were carried out to confirm stationary points as local minima (showing no imaginary frequencies) or transition states (showing one imaginary frequencies) at the same level of theory. The adsoption energy is calculated according to the following equation，

$$\Delta G_{ad}=G(\text{graphene/anion})-G(\text{graphene})-G(\text{anion}) \qquad (S1)$$

The 3D optimized structural figures in this paper were displayed by the CYLview[4] visualization program.

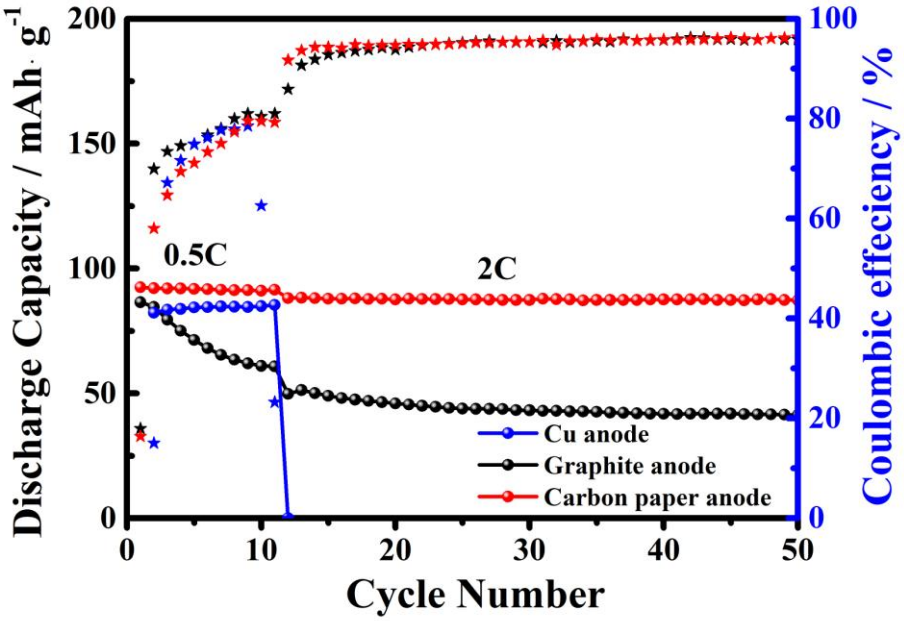

Fig. S1. Performance comparison of Li-free DIBs with Cu, graphite and carbon paper as counter electrode, respectively. Electrolyte: 4M $LiPF_6$+EMC+VC+FEC+ 0.1M LiFSI.

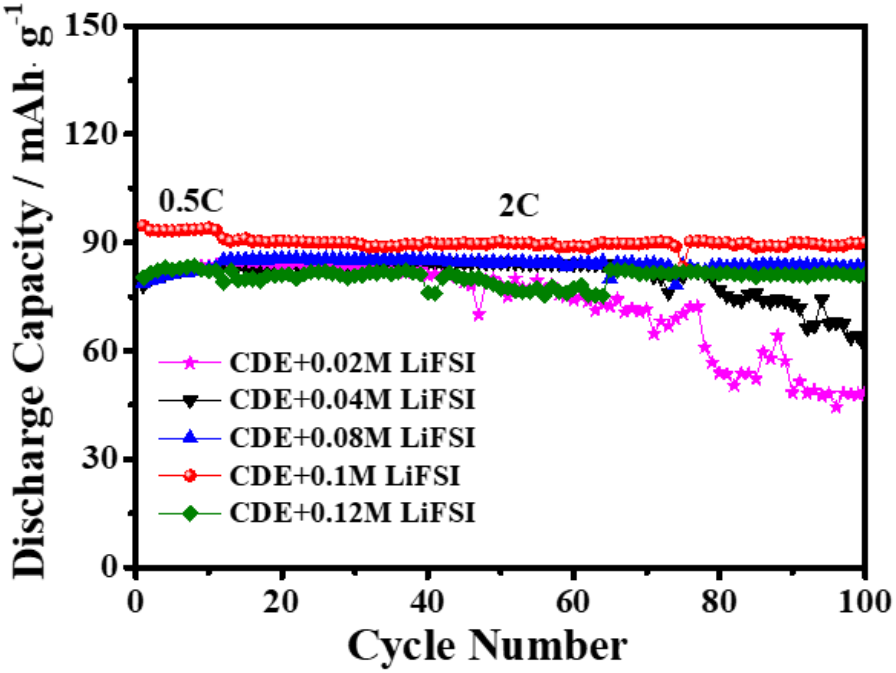

Fig. S2. The cycling performances of Li-free CGDIBs cycled in the electrolyte with different amounts of LiFSI in the voltage range of 3–5 V.

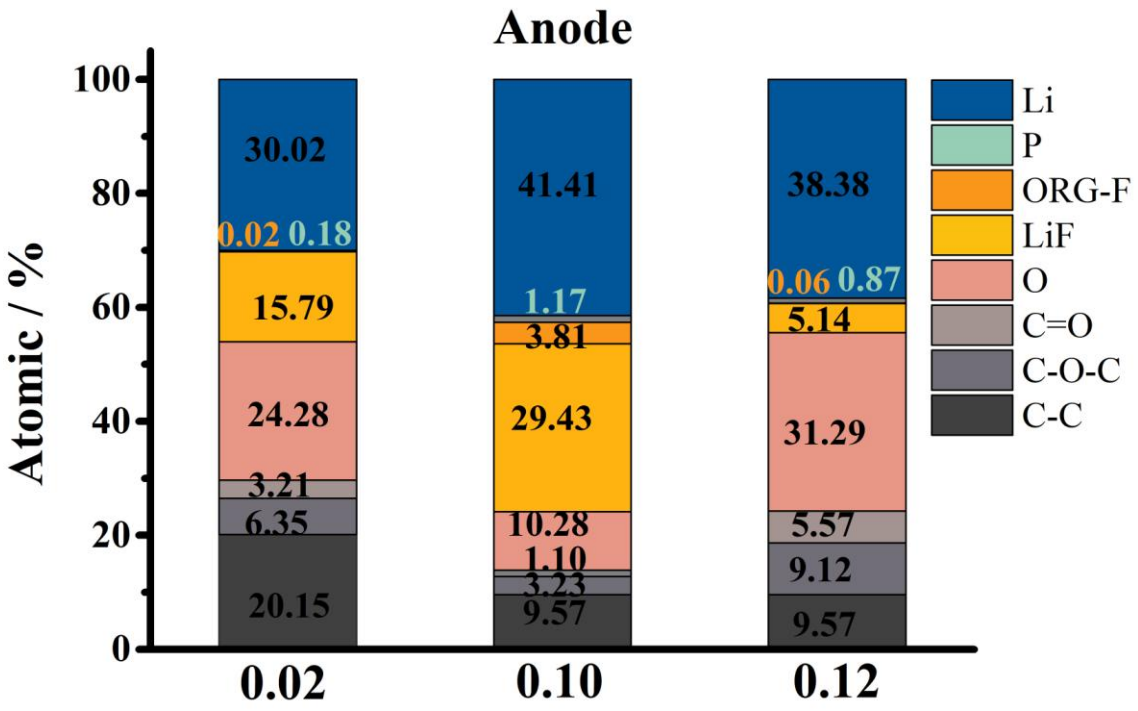

Fig. S3. The atomic percentage of Li, P, F, O, and C in cycled anode from cells after cycling in CDE with different amounts LiFSI for ten cycles.

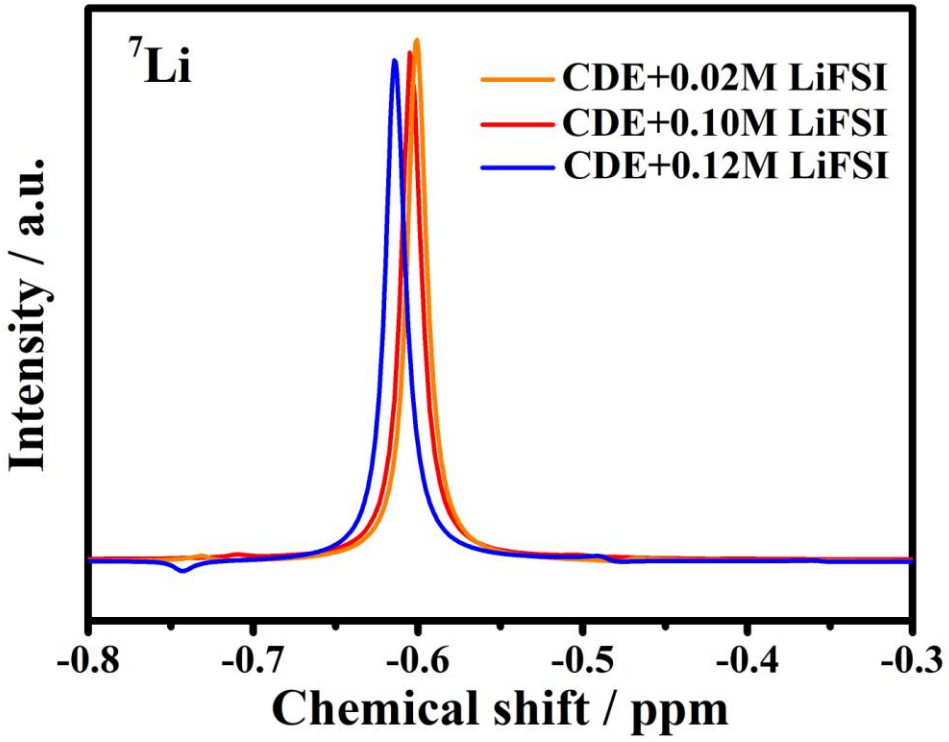

Fig. S4. ^{7}Li NMR spectra of electrolyte with different amounts of LiFSI.

Table S1 Experimental data of the ion conductivity and viscosity of the electrolyte with different amount LiFSI (25℃).

M_{LiFSI}	σ / mS cm^{-1}	η / mPa s
0	2.63	30.01
0.02	2.50	31.82
0.10	2.39	35.01
0.12	2.26	36.12

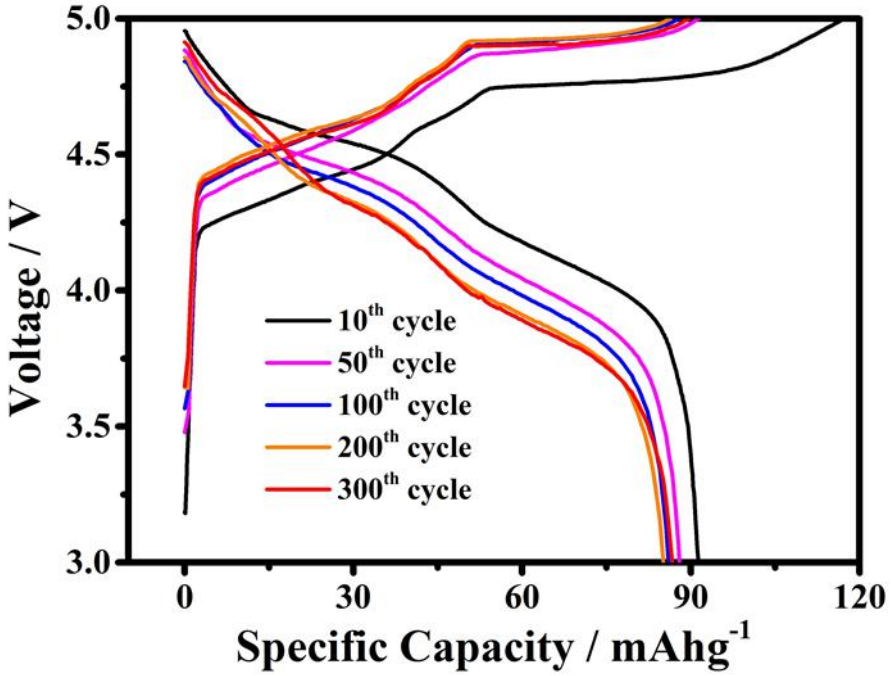

Fig. S5. The corresponding galvanostatic charge/discharge curves of Li-free CGDIBs at different cycles in CDE+LiFSI.

Table S2 Performance comparison of this work and reported DIBs based on various anode materials.

DIB structure	Reversible Capacity (mAh g^{-1}) / current density (mA g^{-1})	capacity retention/ cyclability (cycles)/ current density (mA g^{-1})	Rate capacity (mAh g^{-1}) / current density (mA g^{-1})	Estimated energy density	Reference
Graphite|$LiPF_6$-EMC/ SL| Graphite	93.2 mAh g^{-1} (50 mA g^{-1})	94.7% 1000 (500 mA g^{-1})	88.4 mAh g^{-1} (500 mA g^{-1})	115.6 Wh kg^{-1} (2600.4 W kg^{-1})	[5]
Si/C|$LiPF_6$ -EMC-VC|EG	109.7 mAh g^{-1} (100 mA g^{-1})	78% 1000 (500 mA g^{-1})	96.4 mAh g^{-1} (500 mA g^{-1})	252 Wh kg^{-1} (215 W kg^{-1})	[6]
SEI-modified Li| 4M $LiPF_6$-EMC| graphite	90 mAh g^{-1} (200 mA g^{-1})	89.6% 500 (1000 mA g^{-1})	95.2 mAh g^{-1} (1000 mA g^{-1})		[7]
CNFs-Li|$LiPF_6$-EMC| Graphite	94.4 mAh g^{-1} (200 mA g^{-1})	86.4% 2000 (1000 mA g^{-1})	92.2 mAh g^{-1} (1000 mA g^{-1})		[8]
Li|$LiPF_6$-EMC -$AgPF_6$-$LiNO_3$| Graphite	83 mAh g^{-1} (200 mA g^{-1})	88% 1000 (500 mA g^{-1})	80 mAh g^{-1} (500 mA g^{-1})	374 Wh kg^{-1} (748 W kg^{-1})	[9]
Al|$LiPF_6$-EMC-VC|Graphite	105 mAh g^{-1} (50 mA g^{-1})	88% 200 (200 mA g^{-1})	79 mAh g^{-1} (500 mA g^{-1})	220Wh kg^{-1} (130Wkg^{-1})	[10]
Ge|$LiPF_6$-EC/ DMC |Graphite	281 mAh g^{-1} (250 mA g^{-1})	74.2% 500 (2500 mA g^{-1})	106 mAh g^{-1} (2500 mA g^{-1})		[11]
MnO|$LiPF_6$-EMC-VC |Graphite	104 mAh g^{-1} (100 mA g^{-1})	93% 300 (100 mA g^{-1})	79.6 mAh g^{-1} (500 mA g^{-1})	326 Wh kg^{-1} (326 W kg^{-1})	[12]
MoO_3|$LiPF_6$-EC-DMC|Graphite	81 mAh g^{-1} (100 mA g^{-1})	90% 200 (100 mA g^{-1})		77 Wh kg^{-1}	[13]
Ni_3S_2/Ni foam @ RGO|$LiPF_6$-EMC-VC|Graphite	90 mAh g^{-1} (100 mA g^{-1})	85.6% 500 (100 mA g^{-1})	78 mAh g^{-1} (500 mA g^{-1})		[14]
Carbon paper |$LiPF_6$-EMC-VC-FEC-LiFSI | Graphite	**90 mAh g^{-1} (200 mA g^{-1})**	**89% 500 (500 mA g^{-1})**	**87 mAh g^{-1} (800 mA g^{-1})**	**387 Wh kg^{-1} (450 W kg^{-1})**	**This work**

Calculation method of specific energy density (see reference [10])

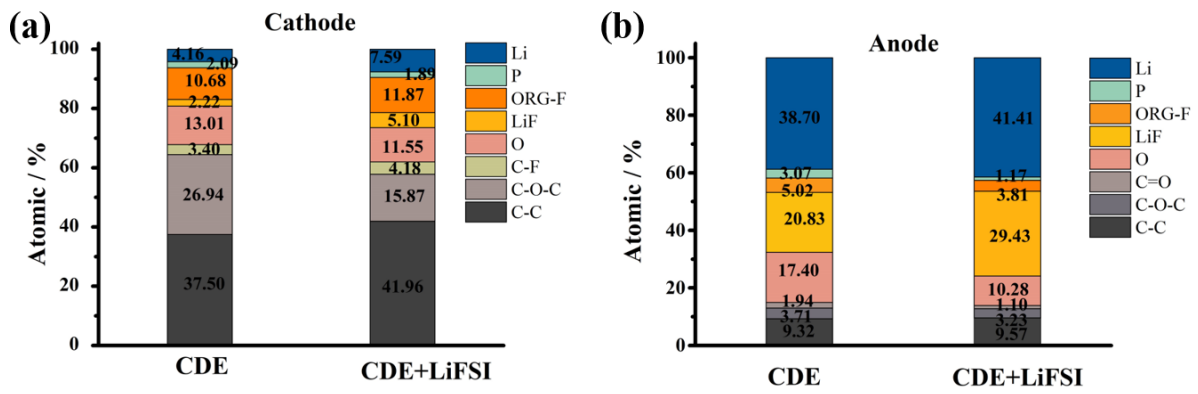

Fig. S6. The atomic percentage of C, P, O, F and Li in cycled cathode and anode electrodes from cells after cycling in CDE and CDE+LiFSI for ten cycles at 0.5 C rate, respectively.

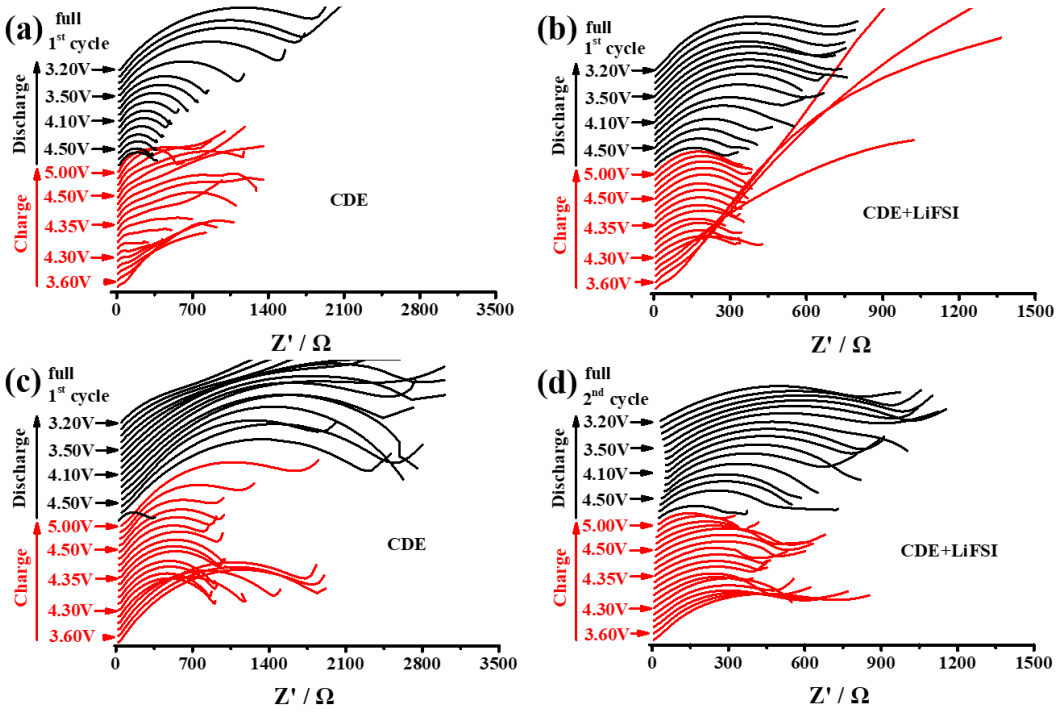

Fig. S7. *In-situ* EIS profiles of Li-free CGDIBs at the initial two cycles in CDE and CDE+ LiFSI.

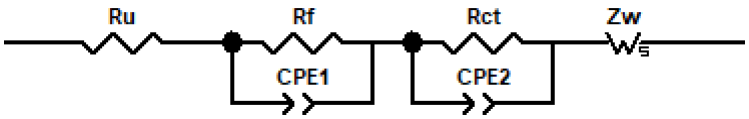

Fig. S8. The equivalent circuit diagram of CGDIBs.

The correlated variations of R_f and R_{ct} are achieved by fitting the Nyquist plots using ZView software.

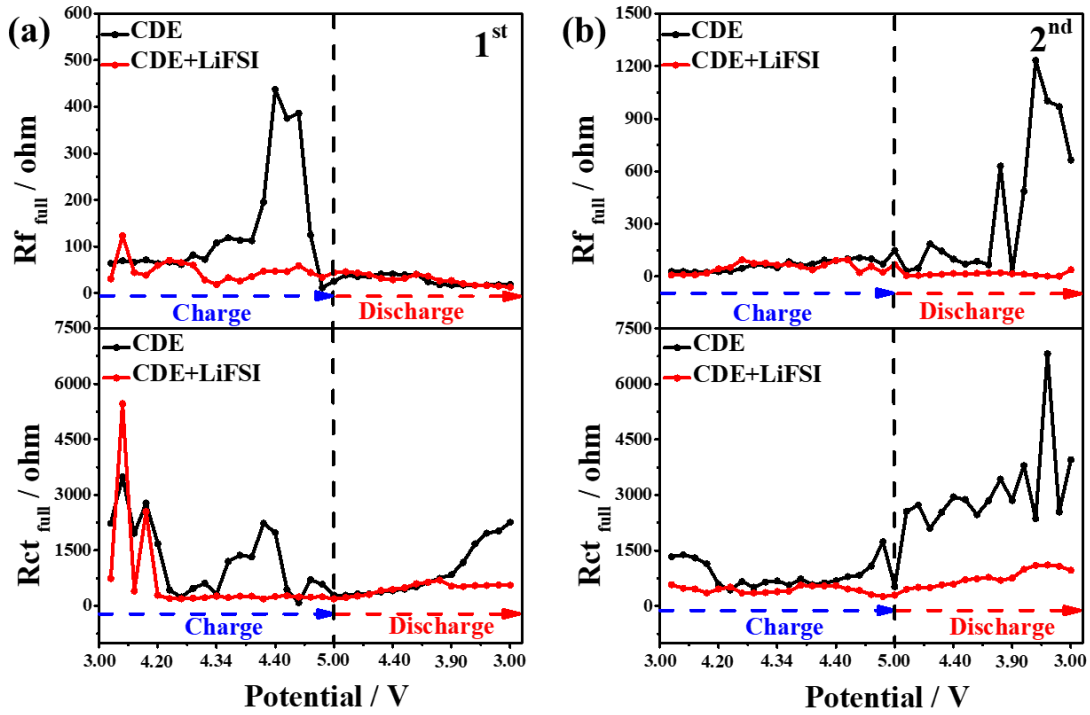

Fig. S9. Variation trend plots of R_f and R_{ct} in the full cell at the initial two cycles in CDE and with CDE+LiFSI.

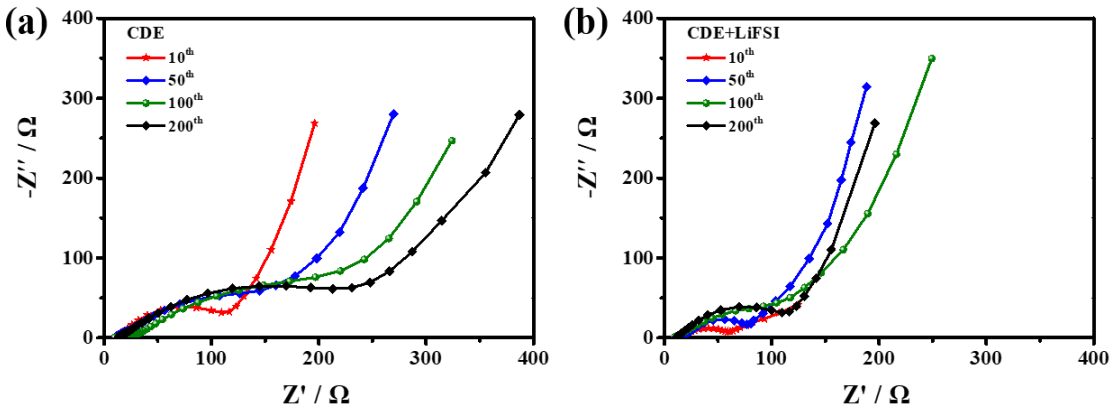

Fig. S10. The EIS impedance spectra of Li-free CGDIBs in different cycles a) in CDE and b) CDE+ LiFSI.

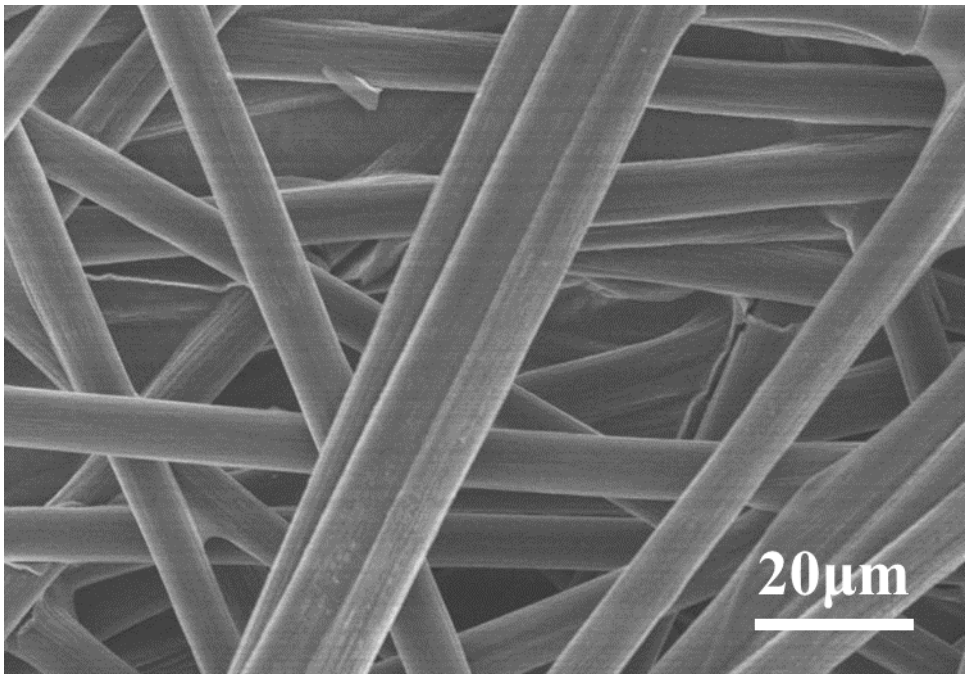

Fig. S11. The SEM image of pure carbon paper material.

Table S3 Overview of the measurement data (2θ values for the most dominant peaks) and calculated parameters [most dominant stage index (n), periodic repeat distance (Ic), gallery height (di), gallery expansion (Δd)] for the operando X-ray diffraction study of PF_6^- anion intercalation/de-intercalation into/from graphite. All data are from Fig. 7.

				CDE			
Cell voltage/V	4.61	4.68	4.66	4.85	4.89	4.98	4.56
2θ(00n+1)/°	25.3	24.55	24.2	24.1/22.95	23	23.05	24.05
2θ(00n+2)/°	29.5	31.2	31.95	32.5/34.6	34.7	34.8	32.35
d(n+2)/d(n+1) ratio	1.16	1.26	1.31	1.34/1.50	1.50	1.50	1.34
Dominant stage(n)	5	3	2	2/1	1	1	2
Periodic repeat distance (Ic) /Å	21.14	14.40	11.11	11.04/7.75	7.73	7.72	11.07
Anion gallery height(di)/Å	7.74	7.70	7.76	7.69/7.75	7.73	7.72	7.72
Anion gallery expansion (Δd) / Å	4.39	4.35	4.41	4.34/4.4	4.38	4.37	4.37
				CDE+LiFSI			
Cell voltage/V	4.63	4.66	4.77	4.88	4.99		4.41
2θ(00n+1)/°	24.8	24.45	24.15	24.05/22.95	24.05/22.95		24
2θ(00n+2)/°	30.7	31.5	32.2	32.5/34.65	32.5/34.65		32.35
d(n+2)/d(n+1) ratio	1.23	1.28	1.32	1.34/1.50	1.34/1.50		1.34
Dominant stage(n)	4	3	2	2/1	2/1		2
Periodicrepeat distance (Ic) /Å	17.69	14.37	11.07	11.05/7.75	7.73		11.08
Anion gallery height(di)/Å	7.64	7.67	7.72	7.70/7.75	7.73		7.73
Anion gallery expansion (Δd) / Å	4.29	4.32	4.37	4.35/4.4	4.38		4.38

References

[1] M. J. Frisch, G. W. Trucks, H. B. Schlegel, G. E. Scuseria, M. A. Robb, J. R. Cheeseman, G. Scalmani, V. Barone, G. A. Petersson, H. Nakatsuji, X. Li, M. Caricato, A. V. Marenich, J. Bloino, B. G. Janesko, R. Gomperts, B. Mennucci, H. P. Hratchian, J. V. Ortiz, A. F. Izmaylov, J. L. Sonnenberg, Williams, F. Ding, F. Lipparini, F. Egidi, J. Goings, B. Peng, A. Petrone, T. Henderson, D. Ranasinghe, V. G. Zakrzewski, J. Gao, N. Rega, G. Zheng, W. Liang, M. Hada, M. Ehara, K. Toyota, R. Fukuda, J. Hasegawa, M. Ishida, T. Nakajima, Y. Honda, O. Kitao, H. Nakai, T. Vreven, K. Throssell, J. A. Montgomery Jr., J. E. Peralta, F. Ogliaro, M. J. Bearpark, J. J. Heyd, E. N. Brothers, K. N. Kudin, V. N. Staroverov, T. A. Keith, R. Kobayashi, J. Normand, K. Raghavachari, A. P. Rendell, J. C. Burant, S. S. Iyengar, J. Tomasi, M. Cossi, J. M. Millam, M. Klene, C. Adamo, R. Cammi, J. W. Ochterski, R. L. Martin, K. Morokuma, O. Farkas, J. B. Foresman, D. J. Fox, **2016**.

[2] Y. Zhao, D. G. Truhlar, *Accounts Chem. Res.* **2008**, *41*, 157.

[3] F. Weigend, R. Ahlrichs, *Phys. Chem. Chem. Phys.* **2005**, *7*, 3297.

[4] C. Y. Legault, *CYLview, 1.0b; , Université de Sherbrooke, 2009*, Online at http://www.cylview.org.

[5] T. Liu, X. Han, Z. Zhang, Z. Chen, P. Wang, P. Han, N. Ding, G. Cui, *J. Power Sources* **2019**, *437*.

[6] S. He, S. Wang, H. Chen, X. Hou, Z. Shao, *J. Mater. Chem. A* **2020**, *8*, 2571.

[7] X.-T. Xi, W.-H. Li, B.-H. Hou, Y. Yang, Z.-Y. Gu, X.-L. Wu, *ACS Appl. Energy Mater.* **2018**, *2*, 201.

[8] X. T. Xi, X. Feng, X. J. Nie, B. H. Hou, W. H. Li, X. Yang, A. B. Yang, W. D. Sun, X. L. Wu, *Chem. Commun.* **2019**, *55*, 8406.

[9] L. N. Wu, J. Peng, F.-M. Han, Y.-K. Sun, T. Sheng, Y.-Y. Li, Y. Zhou, L. Huang, J. T. Li, S. G. Sun, *J. Mater. Chem. A* **2020**, *8*, 4300.

[10] X. L. Zhang, Y. B. Tang, F. Zhang, C. S. Lee, *Adv. Energy Mater.* **2016**, *6*.

[11] J. Zhou, Y. Zhou, X. Zhang, L. Cheng, M. Qian, W. Wei, H. Wang, *Nanoscale* **2020**, *12*, 79.

[12] L. N. Wu, S. Y. Shen, Y. H. Hong, C. H. Shen, F. M. Han, F. Fu, X. D. Zhou, L. Huang, J. T. Li, S. G. Sun, *ACS Appl. Mater. Interfaces* **2019**, *11*, 12570.

[13] N. Gunawardhana, G. J. Park, N. Dimov, A. K. Thapa, H. Nakamura, H. Y. Wang, T. Ishihara, M. Yoshio, *J. Power Sources* **2011**, *196*, 7886.

[14] S. Wang, J. Tu, J. Xiao, J. Zhu, S. Jiao, *J. Energy Chem.* **2019**, *28*, 144.